Cortical Hypometabolism and Crossed Cerebellar Diaschisis Suggest Subcortically Induced Disconnection in CADASIL: An ^{18}F-FDG PET Study

Klaus Tatsch, MD[1]; Walter Koch, MD[1]; Rainer Linke, MD[1]; Gabriele Poepperl, MD[1]; Nils Peters, MD[2]; Markus Holtmannspoetter, MD[3]; and Martin Dichgans, MD[2]

[1]*Department of Nuclear Medicine, Klinikum Grosshadern, Ludwig-Maximilians-University Munich, Munich, Germany;* [2]*Department of Neurology, Klinikum Grosshadern, Ludwig-Maximilians-University Munich, Munich, Germany; and* [3]*Department of Neuroradiology, Klinikum Grosshadern, Ludwig-Maximilians-University Munich, Munich, Germany*

Cerebral autosomal dominant arteriopathy with subcortical infarcts and leukoencephalopathy (CADASIL) is an inherited small-vessel disease caused by mutations in the *NOTCH3* gene. As in sporadic small-vessel disease, ischemic lesions are largely confined to subcortical structures, whereas the cortex is spared. CADASIL, therefore, may serve as a model to study subcortically induced remote effects. The purpose of this study was to evaluate with ^{18}F-FDG PET whether regional cerebral metabolic rate of glucose (rCMRglc) is altered in CADASIL patients and, if so, whether there is evidence of subcortically induced disconnection. **Methods:** Eleven CADASIL patients (7 women, 4 men; mean age, 55.8 ± 6.7 y) without cortical lesions on brain MR images underwent PET after intravenous injection of 120 MBq ^{18}F-FDG, with calculation of rCMRglc according to a previously published method. For further processing, patient studies were registered to a template of a healthy control group and region-of-interest–based and voxelwise comparisons were performed. **Results:** In CADASIL patients, mean rCMRglc was significantly reduced in all cortical and subcortical structures, compared with the values in healthy volunteers. In the subcortical gray matter, metabolic rates, given as the percentage of the mean of healthy volunteers, were 49.7%, 65.3%, and 51.6% in the caudate, putamen, and thalamus, respectively. Among cortical structures, the values were 66.9%, 67.9%, 67.2%, and 76.5% for the frontal, parietal, temporal, and occipital lobes, respectively. On an individual level, most patients showed marked asymmetry and inhomogeneities of cortical glucose metabolism. In 6 (55%) CADASIL patients, there was evidence of crossed cerebellar diaschisis. **Conclusion:** This study showed that cortical glucose metabolism is significantly lower in CADASIL patients than in healthy volunteers. The observed decrease in rCMRglc may in part be explained by a reduction of cerebral blood flow and neuronal loss. In addition, our data provide evidence of remote effects secondary to the functional disruption of subcortical fiber tracts in this particular type of small-vessel disease.

Key Words: CADASIL; cerebral glucose metabolism; ^{18}F-FDG PET; subcortically induced disconnection

J Nucl Med 2003; 44:862–869

Functional disconnection of cortical structures is of particular interest in conditions affecting the subcortical gray and white matter. Cerebral autosomal dominant arteriopathy with subcortical infarcts and leukoencephalopathy (CADASIL) is a genetically defined type of subcortical vascular encephalopathy caused by mutations in the *NOTCH3* gene on chromosome 19 (*1,2*). Major clinical manifestations include recurrent ischemic episodes and progressive cognitive deficits resulting in subcortical dementia (*3,4*). Pathologically, the disease is characterized by lacunar infarcts and incomplete ischemic lesions within subcortical regions (*5*). MRI studies have revealed a microangiopathic pattern of signal abnormalities, including diffuse white-matter hyperintensities in T2 signal and circumscribed subcortical lesions, whereas the cerebral cortex is generally spared (*6,7*).

To our knowledge, only 3 imaging studies have used nuclear medicine techniques on CADASIL patients (*8–10*). Chabriat et al. (*8*) used PET to examine the cerebral blood flow (CBF), oxygen consumption rate, and oxygen extraction fraction of 2 affected individuals. Mellies et al. (*9*) used ethylcysteinate dimer SPECT to study a German CADASIL family. Tuominen (*10*) addressed CBF findings obtained by PET in a homozygous and a heterozygous gene carrier. These reports primarily focused on hemodynamic parameters and were restricted to examinations of single families.

Comparative investigations on patients with vascular dementia have shown that studies of glucose metabolism are more sensitive than studies of CBF in depicting subtle

Received Sep. 3, 2002; revision accepted Feb. 13, 2003.

For correspondence contact: Klaus Tatsch, MD, Department of Nuclear Medicine, Klinikum Grosshadern, Ludwig-Maximilians-University Munich, Marchioninistrasse 15, 81377 Munich, Germany.

E-mail: tatsch@nuk.med.uni-muenchen.de

functional changes (*11–13*). Thus, we decided to use ^{18}F-FDG PET as the primary tool to address possible functional disturbances in CADASIL patients. We hypothesized that cortical glucose metabolism should be reduced in CADASIL patients presenting with subcortical lesions.

MATERIALS AND METHODS

Study Population

Eleven unrelated CADASIL patients (7 women, 4 men; mean age ± SD, 55.8 ± 6.7 y; age range, 46–65 y) were enrolled in this study. For all subjects, the diagnosis had been confirmed by identification of a mutation in the *NOTCH3* gene ($n = 9$) or by skin biopsy ($n = 7$). Clinical assessment included an evaluation of the disability status according to the modified Rankin scale (*14*) and of cognitive performance according to the Mini-Mental State Examination (MMSE) (*15*). In all cases, MR images of the brain were obtained at the time of the PET study. In 7 cases, ^{18}F-FDG PET studies were coregistered to MR images.

^{18}F-FDG PET

^{18}F-FDG PET was performed with an ECAT EXACT HR$^+$ PET scanner (Siemens/CTI). The scanner acquires 63 contiguous transaxial planes, simultaneously covering 15.5 cm of axial field of view. The transaxial and axial resolutions (full width at half maximum) of the PET system were measured as 4.6 mm and 4.0 mm, respectively, at the center and 4.8 mm and 5.4 mm, respectively, at a radial offset of 10 cm. Data acquisition followed a standardized protocol. Each patient was examined in a fasting state with eyes open, with ears plugged, and in a moderately lit environment. The head of the patient was fixed in a foam cushion and adequately positioned in the gantry. Acquisition started with a 15-min transmission scan (^{68}Ge-sources), which was used for subsequent attenuation correction. After the transmission scan, 120 MBq of ^{18}F-FDG were intravenously administered. A PET study was obtained from 30 to 60 min after injection (3 frames, 10 min per frame, 128 × 128 matrix, 3-dimensional acquisition). For further evaluation, the three 10-min frames were added to a single frame comprising the entire 30-min acquisition. Images were reconstructed by filtered backprojection using a Hann filter with a cutoff frequency of 0.5 Nyquist and corrected for scatter and attenuation. A time–activity curve of the ^{18}F-FDG concentration in blood plasma was obtained by sampling arterialized venous blood starting immediately after injection and continuing until 45 min after injection. Venous blood was arterialized using a hot pad (size, 20 cm × 40 cm) placed around the hand (Dyna-Therm; PADI Industrial Trading GmbH). Image voxel values were converted from kBq/cm^3 to micromoles of glucose per 100 g of tissue per minute (μmol/100 g/min) using the methods described by Phelps et al. (*16*), generating a regional cerebral metabolic rate of glucose (rCMRglc). For calculation, the following values were used: lumped constant, 0.52; k1, 0.095; k2, 0.125; k3, 0.069; and k4, 0.0055. For further evaluation, the PET data were transferred to a workstation running the BRASS software (Nuclear Diagnostics) (*17*). It allows registration of a patient's study to a 3-dimensional reference template created from a normal database ($n = 12$; mean age, 33 ± 5 y). The latter was established from ^{18}F-FDG PET studies of healthy volunteers (mostly hospital staff), who underwent a clinical investigation and MRI before the PET scan to exclude neuropsychiatric disorders. Further processing was performed on a voxelwise and regional basis. For voxelwise evaluation, the BRASS program searches voxelwise for clusters of abnormal voxels that meet defined thresholds for size (>0.5 mL) and SD (>2 SD) and can be displayed as a *z* score image. Regional analysis determined the mean rCMRglc within 3-dimensional regions defined by a region-of-interest (ROI) map matched to the template. We used an elaborate ROI map consisting of 63 ROIs covering cortical and subcortical structures (31 symmetric ROIs on each hemisphere; 1 brain stem ROI) defined on the basis of an MR image matched to the normal template. In addition, lobar measurements were obtained by averaging the rCMRglc of the ROIs (composing a lobe) in proportion to their size (number of voxels). Asymmetry indices for ROIs and hemispheres were calculated on the basis of the following formula: (ROI with higher metabolism – corresponding contralateral ROI) divided by the mean of both ROIs (%). In this study, evaluations on a voxelwise and regional basis were used to compare findings in individual CADASIL patients with healthy volunteers, and in addition, groups were compared by creating a template consisting of the patients' examinations.

All subjects gave written informed consent before participation in this study. Patients and healthy volunteers were investigated between 1999 and 2001, with control studies interspersed among patient studies, thus minimizing the effect of possible drifts in rCMRglc measurements over time.

Statistical Analysis

Statistical analysis was performed using SPSS software, version 9.0.1, for Windows (Microsoft). Descriptive PET results are given as mean and SD. Group comparisons between patients and healthy volunteers were performed using a 2-tailed *t* test. *P* values < 0.05 were considered significant.

RESULTS

All CADASIL patients had a history of transient ischemic attacks or stroke. Their scores on the Rankin scale ranged from 0 to 4 (mean, 2.6 ± 1.2), and their MMSE scores were between 13 and 30 (mean, 22 ± 6). Eight of 11 patients presented with psychiatric symptoms (major depression, $n = 4$; adjustment disorder, $n = 4$). All patients had extensive subcortical signal abnormalities on T2- or proton density–weighted MR images in the absence of cortical lesions.

In CADASIL patients, mean rCMRglc was significantly reduced in all cortical and subcortical gray-matter structures, compared with the values in healthy volunteers. Table 1 summarizes the data for the specific lobes and subcortical structures. The metabolic rates were lowest in the subcortical gray matter (thalamus and striatum). Among cortical structures, changes were most pronounced in the frontal, temporal, and parietal cortices, whereas the occipital cortex was slightly less affected. Figure 1 informs in detail about the deviation of the patients from the healthy volunteers in the respective cortical and subcortical structures defined by the ROI map used (mean data for the right and left hemispheres). Data, which are given as the percentage of the mean of the healthy volunteers in the respective ROIs, reached minimal values in the thalamus, basal ganglia, and insula, whereas in cortical structures rCMRglc was comparatively less affected. Focal right-to-left asymmetries were observed in most individuals. Detailed asymmetry indices

TABLE 1
rCMRglc in CADASIL Patients and Healthy Volunteers

Group	Parameter	rCMRglc						
		Frontal	Parietal	Temporal	Occipital	Thalamic	Striatal	Cerebellar
CADASIL	Mean	28.5	29.0	24.8	31.9	20.1	27.3	27.1
	SD	8.1	8.1	6.3	7.2	7.0	6.9	8.0
Control	Mean	42.5	42.7	36.8	41.7	39.0	45.3	37.2
	SD	8.5	8.7	8.1	9.3	9.8	10.4	8.6
	P	<0.001	<0.001	<0.001	<0.01	<0.001	<0.001	<0.01

Data (μmol/100 g/min) are summarized for respective lobes and subcortical structures.

calculated for the respective cortical and subcortical ROIs in patients and healthy volunteers are given in Figure 2. The comparison between the CADASIL and control groups on a pixelwise basis is shown in Figure 3. Corresponding to the ROI-based evaluations, the *z* score image revealed that in the CADASIL group, the highest deviation of rCMRglc from the control group was in the thalamus; striatum; insula; and temporal, frontal, and parietal cortices. Examples of individual patterns of altered rCMRglc are highlighted in Figure 4, which shows the ^{18}F-FDG PET findings in patients with and without clinical impairment (disability and cognitive deficits).

By visual assessment, 6 of 11 CADASIL patients but no healthy volunteers showed marked asymmetry of cerebellar rCMRglc. Asymmetry indices calculated for the cerebellar and cerebral hemispheres of patients and healthy volunteers are summarized in Table 2. As can be seen from the table, patients with visible asymmetry of cerebellar rCMRglc also displayed marked asymmetry of rCMRglc between cerebral hemispheres. In these cases,

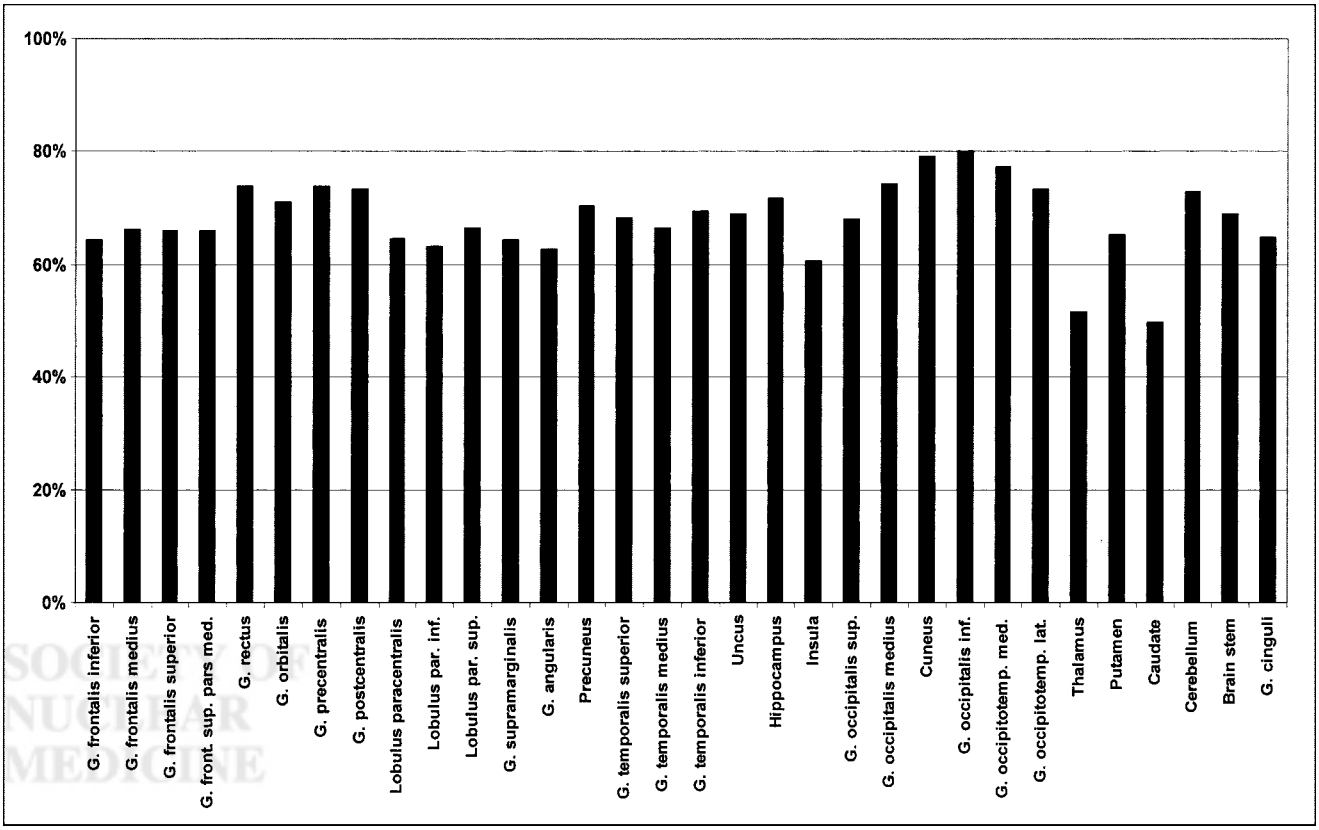

FIGURE 1. ROI analyses of glucose metabolism in CADASIL patients given as percentage of mean of healthy volunteers in cortical and subcortical structures (mean value of corresponding ROIs of right and left hemispheres). Reductions of rCMRglc are most pronounced in subcortical gray matter but are similarly observed in all cortical lobes. front. = frontal; G. = Gyrus; inf. = inferior; lat. = lateral; med. = medial; occipitotemp. = occipitotemporal; par. = parietal; sup. = superior.

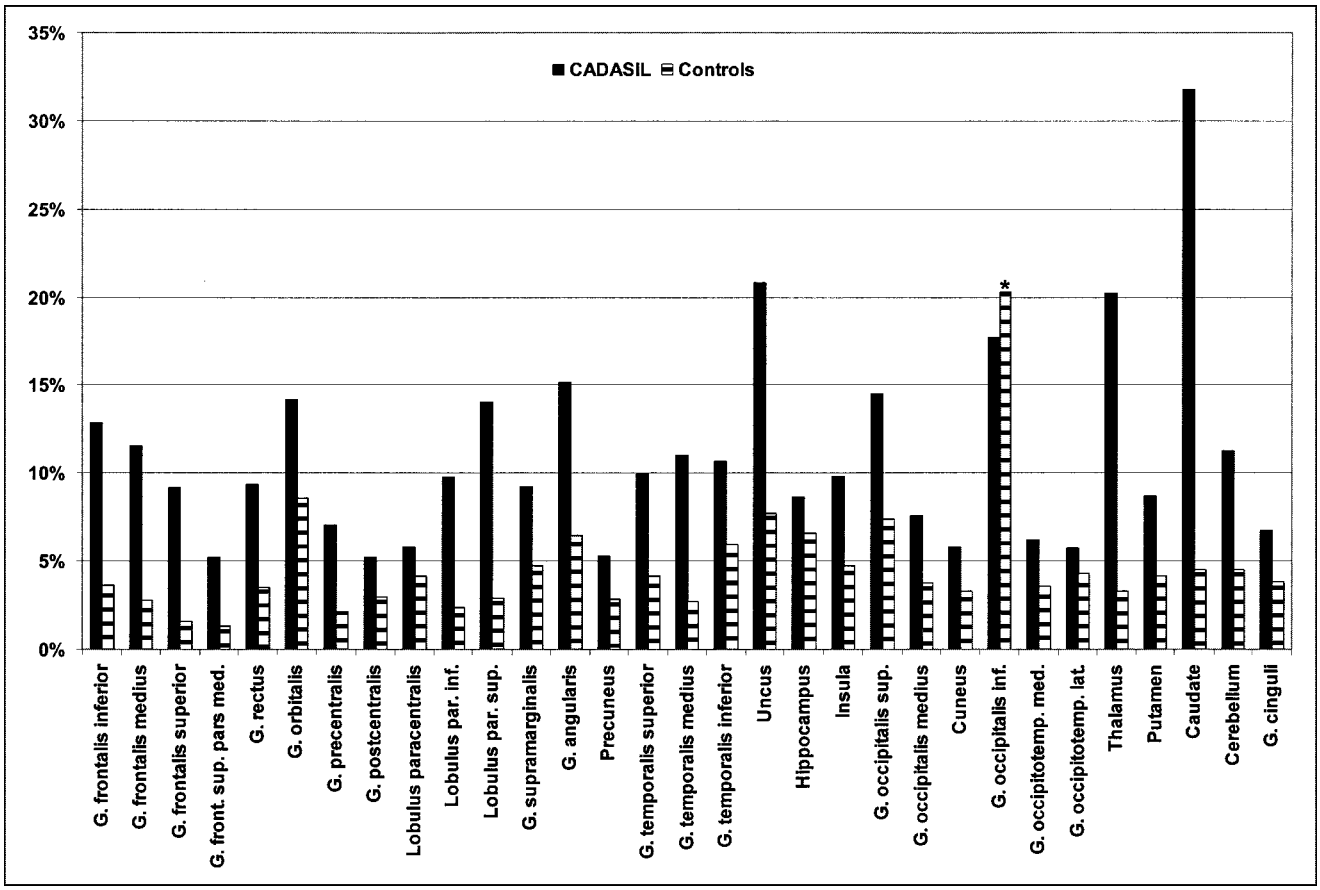

FIGURE 2. Asymmetry indices (%) of glucose metabolism in CADASIL patients and healthy volunteers. Considerably higher asymmetry in patients emphasizes inhomogeneous, focal accentuated character of lesion as also illustrated in case examples in Figures 4 and 5. *High asymmetry index in healthy volunteers in this particularly small ROI was due to structural asymmetry in this ROI in 2 individuals. front. = frontal; G. = Gyrus; inf. = inferior; lat. = lateral; med. = medial; occipitotemp. = occipitotemporal; par. = parietal; sup. = superior.

hypometabolism in one cerebellar hemisphere was always connected with hypometabolism of the contralateral cerebral hemisphere (Table 2). A representative example is shown in Figure 4C. With the exception of one individual, there was no evidence of cerebellar infarction on corresponding MR images. In this particular patient, a small subcortical infarct was revealed in the left caudate and marked hypometabolism was seen in the right cere-

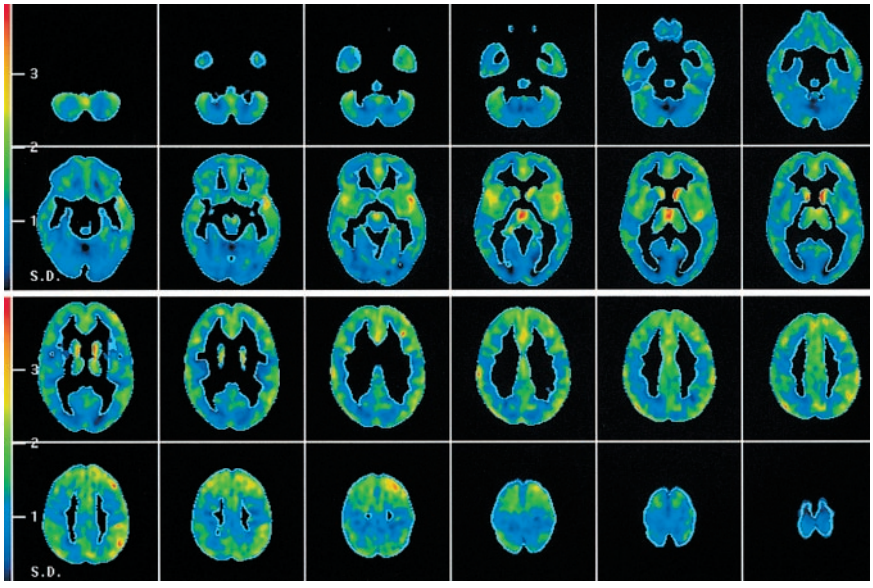

FIGURE 3. Comparison of CADASIL patient group and healthy volunteers. Transverse slices show *z* scores representing, on pixel-by-pixel basis, deviation of patient group from control template. Color scale represents SD and covers range from 0 to 4 SDs. Pixels with reduction of rCMRglc beyond 2 SDs were present in thalamus; striatum; insula; and parts of frontal, temporal, and parietal cortices.

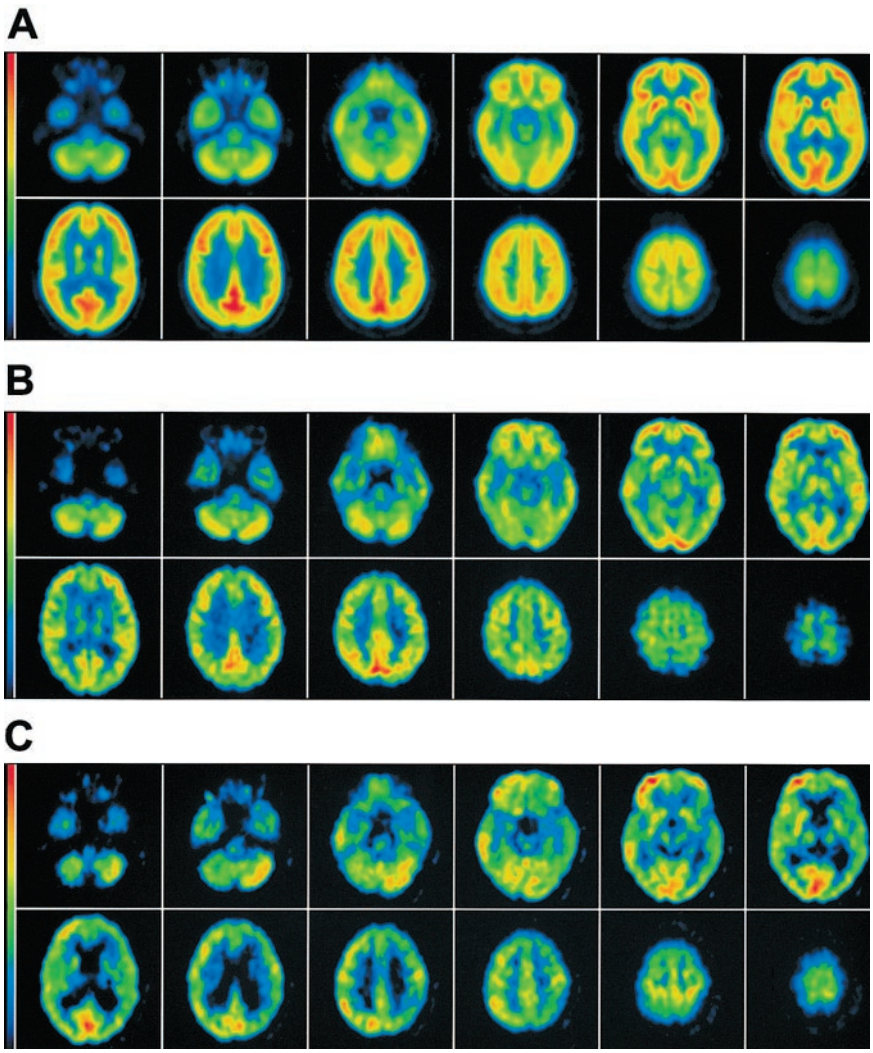

FIGURE 4. Representative examples of characteristic ^{18}F-FDG PET findings in CADASIL patients. (A) Template of control group for comparison. (B) A 64-y-old female CADASIL patient without physical disability (Rankin scale score, 0) or cognitive deficits (MMSE score, 30). In this patient, only moderate reductions of rCMRglc, predominantly in anterior cingulate, temporal lobe, insula, caudate (without marked asymmetry), and left thalamus, were seen. (C) A 50-y-old male CADASIL patient clinically presenting with marked disability (Rankin scale score, 3) and dementia (MMSE score, 14). Pronounced reduction of rCMRglc is seen in frontal, temporal, and parietal cortices (left > right) and in left striatum and thalamus. Metabolism is reduced in right cerebellar hemisphere, suggesting crossed cerebellar diaschisis.

bellar hemisphere, which, however, was contralateral to the cerebellar infarction (Fig. 5).

No significant correlations were observed between cortical glucose metabolism and the Rankin scale score or MMSE score. However, there was a nonsignificant trend toward a correlation between cortical rCMRglc and the MMSE score (frontal cortex: $r = 0.476$, $P = 0.139$; parietal cortex: $r = 0.523$, $P = 0.099$; temporal cortex: $r = 0.427$, $P = 0.190$; occipital cortex: $r = 0.474$, $P = 0.141$).

TABLE 2
Asymmetry Indices of Glucose Metabolism for Cerebellar and Cerebral Hemispheres of Healthy Volunteers and CADASIL Patients

Group	Cerebellar hemisphere	Cerebral hemisphere
Control	4.5	−0.9
CADASIL		
No apparent asymmetry of cerebellar rCMRglc ($n = 5$)	4.3	1.5
Visually apparent asymmetry of cerebellar rCMRglc ($n = 6$)	17.0	−9.1

Data (%) are given as mean reduction in cerebral hemisphere opposite respective cerebellar hemisphere.

DISCUSSION

To our knowledge, this was the first study assessing cerebral glucose metabolism in CADASIL. RCMRglc was found to be significantly lower in CADASIL patients than in healthy volunteers. Changes were most pronounced in the thalamus and striatum. However, a significant reduction of rCMRglc was also found in cortical areas. More important, these changes were observed in the absence of MRI-visible cortical lesions. Fifty-five percent of the patients had evidence of crossed cerebellar diaschisis. Taken together, these findings suggest remote effects caused by subcortical lesions. On an individual level, scattered areas of focal subcortical and cortical hypometabolism were observed, a pattern similar to that found in vascular dementia (*11*,*13*).

At least 3 different mechanisms may account for the metabolic changes in our patients: reduced CBF, neuronal

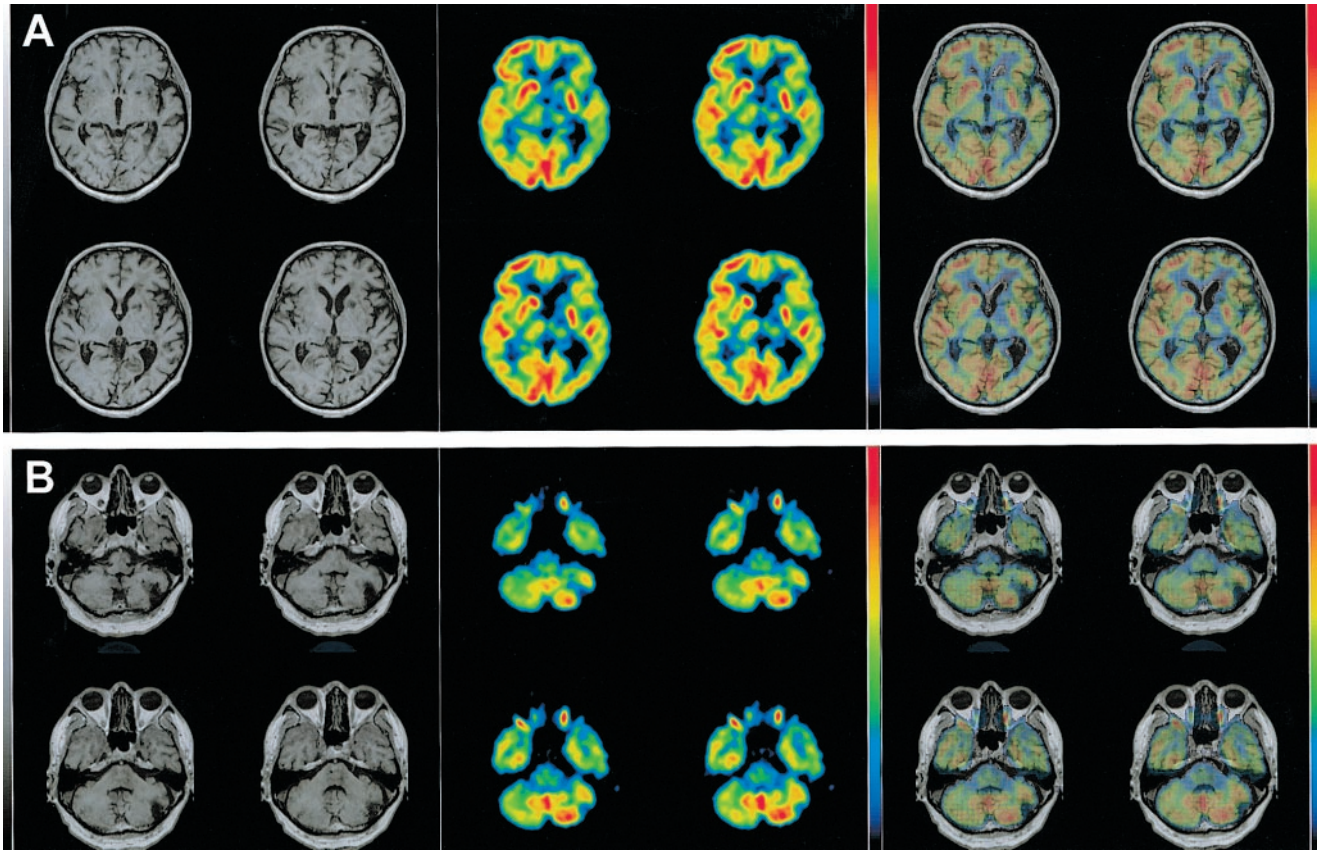

FIGURE 5. Coregistered MR images and ^{18}F-FDG PET scans of 62-y-old male CADASIL patient (Rankin scale score, 2; MMSE score, 15) illustrate structural and functional relationships. (A) Series of 4 consecutive slices at level of basal ganglia. Severe reduction of rCMRglc in left caudate, corresponding to subcortical infarction at this location, also extends into internal capsule. Moderate cortical atrophy but asymmetric glucose metabolism with marked decrease of rCMRglc is seen within left frontal and temporal cortices in absence of cortical infarcts. Left thalamus shows hypometabolism in absence of MRI-visible lesion. (B) Series of 4 consecutive slices at cerebellar level. Vascular lesion is seen in left cerebellar hemisphere, with corresponding defect in PET scan. Overall lower rCMRglc is seen in right cerebellar hemisphere, which shows no visible MRI lesion. In conjunction with observed hypometabolism in left cortex, this finding indicates crossed cerebellar diaschisis.

loss, and functional deactivation secondary to remote lesions in connected brain regions.

A reduction of CBF in CADASIL has been documented using different methodologic approaches. For example, transcranial Doppler sonography has shown that both mean flow velocity in the middle cerebral artery and CO_2 reactivity are reduced (*18*) and that the arteriovenous cerebral transit time is prolonged (*19*) in CADASIL patients. These changes have been connected with the vascular pathology in CADASIL, which affects mainly small arterioles and capillaries. Doppler sonography provides general information on cerebral perfusion but is not suited to assess regional differences in cortical and subcortical blood flow. The latter assessment, however, is mandatory to elucidate the impact of microvascular pathology on cortical perfusion and may be obtained by nuclear medicine techniques.

Using PET, Chabriat et al. found a diffuse 40%–50% decrease in CBF in the cortex and white matter in 2 CADASIL individuals (*8*). Another study, reporting on ethylcysteinate dimer SPECT findings in 6 affected individuals of a German CADASIL family (*9*), observed cortical hypoperfusion that was most pronounced in the frontal and temporal lobes and was less accentuated in the parietal lobe. Finally, Tuominen et al. (*10*) reported significantly reduced cortical blood flow in their PET perfusion studies of a homozygous and heterozygous mutation carrier.

This study assessed cerebral glucose metabolism rather than blood flow. Detailed comparison of our ^{18}F-FDG PET results with the CBF data is hampered by the fact that, in the above studies, quantitative analyses were not extended to all cortical and subcortical structures. With respect to the overall pattern and extent of hypometabolism, our data agree well with the reported CBF changes (*8–10*). However, the relationship between CBF and metabolic changes in CADASIL needs to be made clearer. In general, decreased CBF does not cause decreased metabolism unless there is associated ischemic neuronal damage or unless glucose delivery is so low that increased extraction cannot compensate. Thus, it seems unlikely that the observed reduction of rCMRglc is directly related to decreased CBF. Moreover,

we observed an inhomogeneous, patchy pattern of rCMRglc with marked right-to-left asymmetries in most individuals (Figs. 2, 4, and 5), which is in some contrast to the generalized nature of the underlying angiopathy.

Neuronal loss secondary to ischemia would be another explanation for the reduction of rCMRglc found in cortical and subcortical structures. In fact, several of our patients had lacunar infarcts within the deep nuclei (thalamus and striatum), thus explaining the prominent reduction of rCMRglc in these regions. In cases with coregistered MRI and ^{18}F-FDG PET studies, decreased rCMRglc in subcortical structures often corresponded to the location of small subcortical infarcts (Fig. 4). In contrast, cortical metabolic alterations were seen only in the absence of MRI-visible cortical lesions. Admittedly, we cannot exclude subtle morphologic alterations within the cortex, as were suggested by previous studies using more advanced MRI techniques (*20*–*22*). Also, this pilot study was not designed for a detailed comparison of structural (MRI) and functional (PET) changes. Therefore, we did not apply elaborate methods such as partial-volume or atrophy correction. However, the apparent discrepancy between cortical metabolic and structural alterations suggests mechanisms other than neuronal loss to explain cortical hypometabolism.

A third and attractive explanation for the observed reduction of cortical metabolism is cortical disconnection secondary to subcortical lesions. Of note, subcortical lesions were present in all our patients. Reduced rCMRglc in cortex that is morphologically intact but not afferent is a common finding in ^{18}F-FDG PET (*23*,*24*) and has been discussed as a possible factor in vascular dementia (*13*,*25*). Cortical hypometabolism has further been documented in multiple sclerosis (*26*,*27*), which similarly affects subcortical structures.

Additional evidence for remote effects is provided by the asymmetry in cerebellar glucose metabolism that was observed in 6 of our patients. Of note, cerebellar ischemic lesions were absent in all but one patient—a finding that is in line with previous MRI studies (*6*,*7*). In general, cerebellar hypometabolism was more pronounced contralateral to the more affected cerebral hemisphere, consistent with crossed cerebellar diaschisis. The latter has been attributed mainly to functional disruption of the corticopontocerebellar pathway (*28*).

Corresponding to the widespread white-matter abnormalities, glucose metabolism was reduced in all cortical structures, although slightly less so in the occipital cortex. This pattern agrees well with the known distribution of white-matter signal abnormalities in CADASIL (*6*,*29*,*30*). The distribution of CADASIL white-matter lesions differs from that seen in sporadic small-vessel disease (*29*,*30*). ^{18}F-FDG PET studies directly comparing carriers of the *NOTCH3* mutation with patients having sporadic small-vessel disease may clarify whether there are similar differences in metabolic patterns.

A potential limitation of our study was the difference in age between the CADASIL and control groups. Yet, the extent of rCMRglc reduction in the CADASIL group (20%–50%) largely exceeded the potential influence from age: Between the age of 20 y and the age of 80 y, global metabolic rate has been reported to decrease by approximately 12.5% (*31*). Moreover, phenomena such as regional metabolic differences and right-to-left asymmetries may not be explained by aging effects. Thus, we consider it unlikely that the use of a younger control group would have had a relevant impact on our observations.

This pilot study was not sufficiently powered to detect possible correlations between cortical metabolic changes and clinical parameters. Accordingly, we found no significant correlation between rCMRglc and Rankin score. However, a trend was seen toward a correlation between rCMRglc and the MMSE score. Individual case examples (e.g., Fig. 3) demonstrated a more prominent reduction of rCMRglc in demented patients than in subjects with little or no impairment. The idea that cortical hypometabolism reflects clinically relevant subcortically induced disconnection is in line with recent MRI studies showing that quantitative measures of subcortical pathology in CADASIL are related to cognitive dysfunction (*20*–*22*,*32*). Furthermore, metabolic studies in sporadic small-vessel disease (*33*) and vascular dementia (*11*,*25*) have shown that the extent of cortical hypometabolism is related to cognitive function.

CONCLUSION

This study demonstrated that cortical and subcortical glucose metabolism is severely reduced in patients with CADASIL. Our data suggest an important role for remote cortical effects secondary to subcortical lesions in CADASIL, a genetic variant of cerebral small-vessel disease.

REFERENCES

1. Tournier-Lasserve E, Joutel A, Melki J, et al. Cerebral autosomal dominant arteriopathy with subcortical infarcts and leukoencephalopathy maps to chromosome 19q12. *Nat Genet.* 1993;3:256–259.
2. Joutel A, Corpechot C, Ducros A, et al. Notch3 mutations in CADASIL, a hereditary adult-onset condition causing stroke and dementia. *Nature.* 1996;383:707–710.
3. Chabriat H, Vahedi K, Iba-Zizen MT, et al. Clinical spectrum of CADASIL: a study of 7 families—cerebral autosomal dominant arteriopathy with subcortical infarcts and leukoencephalopathy. *Lancet.* 1995;346:934–939.
4. Dichgans M, Mayer M, Uttner I, et al. The phenotypic spectrum of CADASIL: clinical findings in 102 cases. *Ann Neurol.* 1998;44:731–739.
5. Ruchoux MM, Maurage CA. CADASIL: cerebral autosomal dominant arteriopathy with subcortical infarcts and leukoencephalopathy. *J Neuropath Exp Neurol.* 1997;56:947–964.
6. Chabriat H, Levy C, Taillia H, et al. Patterns of MRI lesions in CADASIL. *Neurology.* 1998;51:452–457.
7. Coulthard A, Blank SC, Bushby K, Kalaria RN, Burn DJ. Distribution of cranial MRI abnormalities in patients with symptomatic and subclinical CADASIL. *Br J Radiol.* 2000;73:256–265.
8. Chabriat H, Bousser MG, Pappata S. Cerebral autosomal dominant arteriopathy with subcortical infarcts and leucoencephalopathy: a positron emission tomography study in two affected family members [letter]. *Stroke.* 1995;26:1729–1730.
9. Mellies JK, Bäumer T, Müller JA, et al. SPECT study of a German CADASIL family. *Neurology.* 1998;50:1715–1721.

10. Tuominen S, Juvonen V, Amberla K, et al. Phenotype of a homozygous CADASIL patient in comparison to 9 age-matched heterozygous patients with the same R133C *Notch3* mutation. *Stroke.* 2001;32:1767–1774.
11. Mielke R, Kessler J, Szelies B, Herholz K, Wienhard K, Heiss WD. Vascular dementia: perfusional and metabolic disturbances and effects of therapy. *J Neural Transm Suppl.* 1996;47:183–191.
12. Mielke R, Heiss WD. Positron emission tomography for diagnosis of Alzheimer's disease and vascular dementia. *J Neural Transm Suppl.* 1998;53:237–250.
13. Mielke R, Pietrzyk U, Jacobs A, et al. HMPAO SPET and FDG PET in Alzheimer's disease and vascular dementia: comparison of perfusion and metabolic pattern. *Eur J Nucl Med.* 1994;21:1052–1060.
14. de Haan R, Limburg M, Bossuyt P, van der Meulen J, Aaronson N. The clinical meaning of Rankin 'handicap' grades after stroke. *Stroke.* 1995;26:2027–2030.
15. Folstein MF, Folstein SE, McHugh PR. "Mini-mental state": a practical method for grading the cognitive state of patients for the clinician. *J Psychiatr Res.* 1975;12:189–198.
16. Phelps ME, Hunag SC, Hoffman EJ, Selin C, Sokoloff L, Kuhl DE. Tomographic measurement of local cerebral glucose metabolic rate in human with (F-18)2-fluoro-2-deoxy-D-glucose: validation of method. *Ann Neurol.* 1979;6:371–388.
17. Slomka PJ, Radau P, Hurwitz GA, Dey D. Automated three-dimensional quantification of myocardial perfusion and brain SPECT. *Comput Med Imaging Graph.* 2001;25:153–164.
18. Pfefferkorn T, von Stuckrad-Barre S, Herzog J, Gasser T, Hamann GF, Dichgans M. Reduced cerebrovascular CO_2 reactivity in CADASIL: a transcranial Doppler sonography study. *Stroke.* 2001;32:17–21.
19. Liebetrau M, Herzog J, Kloss CU, Hamann GF, Dichgans M. Prolonged cerebral transit time in CADASIL: a transcranial ultrasound study. *Stroke.* 2002;33:509–512.
20. Auer DP, Schirmer T, Heidenreich JO, Herzog J, Putz B, Dichgans M. Altered white and gray matter metabolism in CADASIL: a proton MR spectroscopy and 1H-MRSI study. *Neurology.* 2001;56:635–642.
21. Iannucci G, Dichgans M, Rovaris M, et al. Correlations between clinical findings and magnetization transfer imaging metrics of tissue damage in individuals with cerebral autosomal dominant arteriopathy with subcortical infarcts and leukoencephalopathy. *Stroke.* 2001;32:643–648.
22. Chabriat H, Pappata S, Poupon C, et al. Clinical severity in CADASIL related to ultrastructural damage in white matter: in vivo study with diffusion tensor MRI. *Stroke.* 1999;30:2637–2643.
23. Kuhl DE, Phelps ME, Kowell AP, Metter EJ, Selin C, Winter J. Effects of stroke on local cerebral metabolism and perfusion: mapping by emission computed tomography of ^{18}FDG and ^{13}NH3. *Ann Neurol.* 1980;8:47–60.
24. Heiss WD, Ilsen HW, Wagner R, Pawlik G, Wienhard K, Eriksson L. Remote functional depression of glucose metabolism in stroke and its alterations by activating drugs. In: Heiss WD, Phelps ME, eds. *Positron Emission Tomography of the Brain.* Berlin, Germany: Springer; 1983:162–168.
25. Sultzer DL, Mahler ME, Cummings JL, Van Gorp WG, Hinkin CH, Brown C. Cortical abnormalities associated with subcortical lesions in vascular dementia: clinical and positron emission tomographic findings. *Arch Neurol.* 1995;52:773–780.
26. Blinkenberg M, Rune K, Jensen CV, et al. Cortical cerebral metabolism correlates with MRI lesion load and cognitive dysfunction in MS. *Neurology.* 2000;54:558–564.
27. Roelcke U, Kappos L, Lechner-Scott J, et al. Reduced glucose metabolism in the frontal cortex and basal ganglia of multiple sclerosis patients with fatigue: a ^{18}F-fluorodeoxyglucose positron emission tomography study. *Neurology.* 1997;48:1566–1571.
28. Fulham MJ, Brooks RA, Hallett M, Di Chiro G. Cerebellar diaschisis revisited: pontine hypometabolism and dentate sparing. *Neurology.* 1992;42:2267–2273.
29. Auer DP, Puetz B, Goessl C, Elbel GK, Gasser T, Dichgans M. Differential lesion patterns in CADASIL and sporadic subcortical arteriosclerotic encephalopathy: MR imaging study with statistical parametric group comparison. *Radiology.* 2001;218:443–451.
30. O'Sullivan M, Jarosz JM, Martin RJ, Deasy N, Powell JF, Markus HS. MRI hyperintensities of the temporal lobe and external capsule in patients with CADASIL. *Neurology.* 2001;56:628–634.
31. Moeller JR, Ishikawa T, Dhawan V, et al. The metabolic topography of normal aging. *J Cereb Blood Flow Metab.* 1996;16:385–398.
32. Dichgans M, Filippi M, Bruening R, et al. Quantitative MRI in CADASIL: correlation with disability and cognitive performance. *Neurology.* 1999;52:1361–1367.
33. Sabri O, Hellwig D, Schreckenberger M, et al. Correlation of neuropsychological, morphological and functional (regional CBF and glucose use) findings in cerebral microangiopathy. *J Nucl Med.* 1998;39:147–154.

JNM The Journal of NUCLEAR MEDICINE

Cortical Hypometabolism and Crossed Cerebellar Diaschisis Suggest Subcortically Induced Disconnection in CADASIL: An ^{18}F-FDG PET Study

Klaus Tatsch, Walter Koch, Rainer Linke, Gabriele Poepperl, Nils Peters, Markus Holtmannspoetter and Martin Dichgans

J Nucl Med. 2003;44:862-869.

The Journal of Nuclear Medicine is published monthly.
SNMMI | Society of Nuclear Medicine and Molecular Imaging
1850 Samuel Morse Drive, Reston, VA 20190.
(Print ISSN: 0161-5505, Online ISSN: 2159-662X)

SNMMI SOCIETY OF NUCLEAR MEDICINE AND MOLECULAR IMAGING